



Contents lists available at ScienceDirect

# Journal of Quantitative Spectroscopy & Radiative Transfer

journal homepage: [www.elsevier.com/locate/jqsrt](http://www.elsevier.com/locate/jqsrt)

## First measurements of the HCFC-142b trend from atmospheric chemistry experiment (ACE) solar occultation spectra

Curtis P. Rinsland<sup>a,\*</sup>, Linda Chiou<sup>b</sup>, Chris Boone<sup>c</sup>, Peter Bernath<sup>d</sup>, Emmanuel Mahieu<sup>e</sup><sup>a</sup> NASA Langley Research Center, Hampton, VA, USA<sup>b</sup> Science Systems and Applications, Inc., Hampton, VA, USA<sup>c</sup> Department of Chemistry, University of Waterloo, Waterloo, Ontario, Canada N2L 3G1<sup>d</sup> Department of Chemistry, University of York, Heslington, York YO10 5DD, UK<sup>e</sup> Institute of Astrophysics and Geophysics, University of Liège, Liège, Belgium

### ARTICLE INFO

#### Article history:

Received 31 March 2009

Received in revised form

15 May 2009

Accepted 19 May 2009

#### Keywords:

Remote sensing

Atmospheric chemistry

Composition

Hydrochlorofluorocarbons

Trends

Ozone depletion

### ABSTRACT

The first measurement of the HCFC-142b ( $\text{CH}_3\text{CClF}_2$ ) trend near the tropopause has been derived from volume mixing ratio (VMR) measurements at northern and southern hemisphere mid-latitudes for the 2004–2008 time period from spaceborne solar occultation observations recorded at  $0.02\text{ cm}^{-1}$  resolution with the ACE (atmospheric chemistry experiment) Fourier transform spectrometer. The HCFC-142b molecule is currently the third most abundant HCFC (hydrochlorofluorocarbon) in the atmosphere and ACE measurements over this time span show a continuous rise in its volume mixing ratio. Monthly average measurements at northern and southern hemisphere mid-latitudes have similar increase rates that are consistent with surface trend measurements for a similar time span. A mean northern hemisphere profile for the time span shows a near constant VMR at 8–20 km altitude range, consistent on average for the same time span with *in situ* results. The nearly constant vertical VMR profile also agrees with model predictions of a long lifetime in the lower atmosphere.

© 2009 Elsevier Ltd. All rights reserved.

### 1. Introduction

The phase out of fully fluorinated chlorofluorocarbons (CFCs) mandated by the Montreal Protocol on substances that deplete the ozone layer [1] and its subsequent amendments [2] has prompted the use of temporary hydrochlorofluorocarbon replacements including HCFC-142b ( $\text{CH}_3\text{CClF}_2$ ). At present, it is the third most abundant HCFC in the atmosphere, after HCFC-22 ( $\text{CHClF}_2$ ) and HCFC-141b ( $\text{C}_2\text{H}_3\text{Cl}_2\text{F}$ ), though a decrease in its emission rate (weighted by ozone depletion potential) in 2000 was noted in recent World Meteorological Organization (WMO) reports [3,4]. Subsequently, an accelerated rate of accumulation has been reported for all three HCFCs after 2004 [5]. The hydrochlorofluorocarbon replacement molecules are mainly used as a refrigerant, solvent, and an aerosol propellant in foams. The primary use of HCFC-142b is in foams, largely replacing CFC-11 ( $\text{CCl}_3\text{F}$ ). The lifetime of HCFC-142b is estimated as 20.1 yr in the troposphere and 146 yr in the stratosphere assuming its total atmospheric burden and loss rate for 2000 emissions based on a box model and loss due to reaction with OH [4]. A similar minimum stratospheric lifetime of  $138 \pm 29$  yr was obtained based on a linear tracer-tracer correlation using whole-air sampling measurements and assuming an  $\text{N}_2\text{O}$  stratospheric

\* Corresponding author. Tel.: +1757 8642699; fax: +1757 8648197.

E-mail addresses: [curtis.p.rinsland@nasa.gov](mailto:curtis.p.rinsland@nasa.gov) (C.P. Rinsland), [linda.s.chiou@nasa.gov](mailto:linda.s.chiou@nasa.gov) (L. Chiou), [cboone@sciborg.uwaterloo.ca](mailto:cboone@sciborg.uwaterloo.ca) (C. Boone), [bernath@uwaterloo.ca](mailto:bernath@uwaterloo.ca), [pfb500@york.ac.uk](mailto:pfb500@york.ac.uk) (P. Bernath), [emmanuel.mahieu@ulg.ac.be](mailto:emmanuel.mahieu@ulg.ac.be) (E. Mahieu).

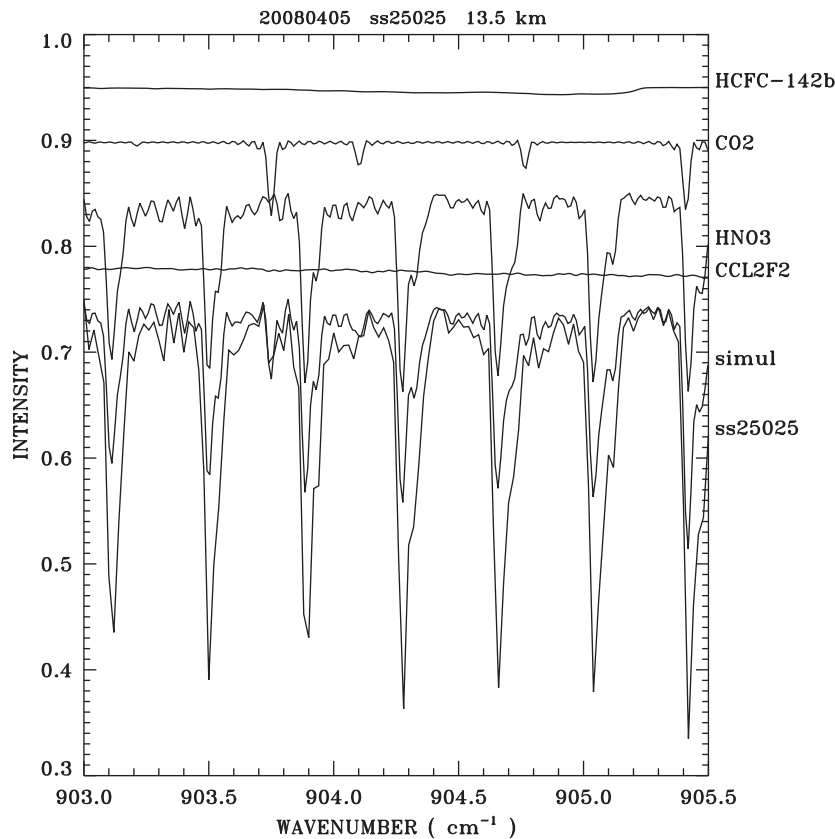


**Fig. 1.** Simulation of the HCFC-142b  $\nu_7$  band Q branch region for the most significant absorption features and an ACE spectrum recorded at 27.78°N latitude and 37.05°W longitude on April 5, 2008. The simulated and measured spectra are normalized and offset vertically for clarity and the version 2.2 tangent altitude is indicated at top.

lifetime of 110 yr [6]. The detection and first remote sensing measurement of HCFC-142b volume mixing ratio (VMR) profiles were reported based on infrared solar occultation spectra covering altitudes of 8–15 km [7] from measurements recorded by the Atmospheric Chemistry Experiment (ACE) Fourier transform spectrometer (FTS) [8]. A nearly uniform VMR of 15 pptv ( $10^{-12}$  per unit volume) was reported based on measurements from 12 mid-latitude occultations recorded around 53°N latitude on 26 and 27 March 2004, along with 5 occultations recorded in the tropics (25°S–25°N) between 31 January and 8 February 2004. The retrieved VMR for January–March 2004 was compared and found to be consistent with the AGAGE (Advanced Global Atmospheric Gases Experiment) surface VMRs measured at 53°N latitude from the station at Mace Head, Ireland, with differences less than 10% on average for the three mid-latitude measurements and less than 15% for the tropical measurements. As noted in [4,5,7], measurements of HCFC-142b are also obtained by NOAA's Earth System Research Laboratory (ESRL) with differences of ~5% for time coincident flask sampling measurements (see Fig. 1 of Ref. [4]). The two microwindows for the ACE retrieval [7] were 1132.5–1136.5 and 1191.5–1195.5  $\text{cm}^{-1}$  and were slightly broader than the selections recommended earlier in a study that first predicted the feasibility of HCFC-142b detection by remote sensing from space [9]. The purpose of this paper is to report the first time series of HCFC-142b measurements at 13–16 km altitude obtained with the ACE-FTS at mid-latitudes in both hemispheres and their comparison with mid-latitude surface station measurements at similar latitudes for 2004–2008.

## 2. Measurements

The Atmospheric Chemistry Experiment, also known as SCISAT-1, is a Canadian-led mission for atmospheric remote sensing launched on 12 August 2003 into a 74° inclined orbit at 650 km altitude by a NASA-supplied Pegasus XL rocket [8]. Three instruments with a shared field of view record high resolution atmospheric spectra taking advantage of the high precision of the solar occultation technique. An infrared Fourier transform spectrometer records solar spectra below 150 km altitude at 0.02  $\text{cm}^{-1}$  spectral resolution (maximum optical path difference of  $\pm 25$  cm) from 750 to 4400  $\text{cm}^{-1}$ . Photovoltaic detectors with near linear response produce a signal-to-noise ratio  $> 300$  throughout most of the infrared. Full resolution spectra are recorded in 2 s with an altitude spacing determined by the scan time, typically 3–4 km, varying from 2 km for high beta angle (angle between the satellite velocity vector and the vector to the Sun) occultations to 6 km for zero

beta angle occultations. As a result of refraction, tangent altitude spacing is typically less than 2 km in the troposphere. The FTS has a circular field of view of 1.25 mrad ( $10^{-3}$  rad) diameter; it is self-calibrating as linear response photovoltaic detectors are used and low Sun solar occultation spectra are divided by exo-atmospheric solar spectra from the same occultation. Limited seasonal and latitudinal sampling is obtained as the orbit is optimized for high latitude coverage in both hemispheres. Additional scientific instruments are a dual channel UV–visible spectrometer and imagers with optical filters at 0.525 and 1.02  $\mu\text{m}$ .

### 3. Analysis

Measurements of temperature and pressure dependent infrared cross sections of HCFC-142b vapor have been reported in numerous laboratory studies (e.g. [10–14]). The strongest bands occur in the thermal infrared covered by ACE-FTS measurements. Vibrational assignments show the  $\nu_7$  band at  $904\text{ cm}^{-1}$  and other bands in the thermal infrared have prominent central Q branches. Although it is the weakest in integrated intensity by about a factor of three among the strongest bands, the  $\nu_7$  band occurs in an open spectral region with few interfering molecules as compared to the other regions used in the previous retrievals [7]. Our analysis assumes a line list (“pseudo lines”) that has been generated from laboratory cross sections (G. C. Toon, Jet Propulsion Laboratory, private communication, 2006). The procedure is widely used for atmospheric retrievals from ground-based solar spectra and was also been used for retrievals from balloon-borne and solar occultation spectra recorded with the ATMOS (Atmospheric Trace MOlecule Spectroscopy) FTS [15]. All of the relevant laboratory transmittance spectra were fitted simultaneously while solving for the 296 K intensity and the ground state energy ( $E''$ ) of each pseudo-line assuming a Boltzmann distribution including the variations with temperature of the rotational and vibrational partition function and stimulated emission [16]. The procedure to generate the pseudolines assumes all lines in a given absorption band have the same pressure-broadened halfwidth and the same halfwidth dependence on temperature. The pseudo-line list was generated from the cross section measurements of Newnham and Ballard [10], which were measured at temperatures of 203, 213, 233, 253, 273, and 294 K and cover  $870\text{--}1270\text{ cm}^{-1}$  with a line spacing of  $0.010\text{ cm}^{-1}$ . A maximum error of 4% in absorber was found by refitting the laboratory spectra using the final pseudo-linelist. A coefficient of 1.5 was assumed for the temperature dependence of the rotational partition function. The vibrational partition function was calculated assuming the frequencies of the 18 modes of the HCFC-142b molecule [11–14]. Fig. 1 presents a simulation of the interval used for atmospheric retrievals,  $903.0\text{--}905.5\text{ cm}^{-1}$  for a tangent altitude of 13.526 km. A measured ACE spectrum and simulations for the most important molecules are normalized and offset vertically for clarity. As can be seen from this plot, the HCFC-142b Q branch feature is predicted to be weak but detectable with the interval dominated by strong features of  $\text{CO}_2$  and  $\text{HNO}_3$  in addition to weaker absorption by  $\text{CCl}_2\text{F}_2$  (CFC-12). It should be noted that the pseudo-line list we have assumed differs from the data in HITRAN 2004 [18], which was limited to HCFC-142b cross section measurements at three temperatures based on the measurements of Clerbaux et al. [12] with the same set of cross sections provided in HITRAN 2008 [19].

Atmospheric retrievals were performed for HCFC-142b based on the window shown in Fig. 1 for solar occultations at mid-latitudes in the northern and southern hemisphere. The interval displayed in Fig. 1 was fitted for HCFC-142b,  $\text{CO}_2$ ,  $\text{HNO}_3$ , and  $\text{CCl}_2\text{F}_2$  simultaneously with a multi-microwindow Levenberg–Marquardt nonlinear least-squares global-fitting technique [17]. Except for the pseudo-lines of HCFC-142b and  $\text{CCl}_2\text{F}_2$  (CFC-12), which also occur in the spectral interval, concentration profiles were retrieved from simultaneous fits to sequences of spectra over pre-selected altitude ranges to derive the profile of the target species using the HITRAN 2004 molecular spectroscopic parameters [18] and assuming a set of realistic *a priori* VMR profiles for the target and interfering species. The analysis approach is the same as is used to retrieve profiles from ACE spectra [20], though HCFC-142b profiles are not currently reported by ACE for the measurement of time span. We also assumed temperature and tangent altitudes derived from version 2.2 ACE spectra [20].

### 4. Results and discussion

Fig. 2 represents a fit to the same sample ACE occultation as shown in Fig. 1. The top panel displays the measured minus calculated spectrum on an expanded vertical scale, fitting  $\text{CO}_2$ ,  $\text{HNO}_3$ , and  $\text{CCl}_2\text{F}_2$  as interferences. As shown by this typical example, the measurements are fitted to close to the noise level in the measured spectrum. The normalized measured spectrum is displayed in the lower panel. The second residual plot shows the fit obtained with HCFC-142b set to zero. The broad HCFC-142b Q branch feature can be noted. The third residual plot shows the HCFC-142b contribution calculated as the difference between the residuals obtained while excluding or including the HCFC-142b contribution. The comparison with the measured spectrum shows coincidences with locations of strong  $\text{HNO}_3$  features in the difference spectrum. As  $\text{HNO}_3$  is a major absorber in the region, we concluded it is not accurately modeled, probably because of limitations to the spectroscopic parameters for  $\text{HNO}_3$  in the HITRAN 2004 database [18]. More accurate positions, intensities, and rotationally-dependent air-broadening parameters for  $\text{HNO}_3$  and approximate parameters for two hot bands have recently been incorporated in the HITRAN 2008 database [19].

Fig. 3 (upper panel) illustrates the time series comparison of ACE monthly mean HCFC-142b VMR measurements averaged over altitudes of 13–16 km for latitudes of  $25\text{--}35^\circ\text{N}$  and  $25\text{--}35^\circ\text{S}$ , between February 2004 to August 2008. Corresponding measurements from two AGAGE surface stations are shown in the lower panel, for approximately the same

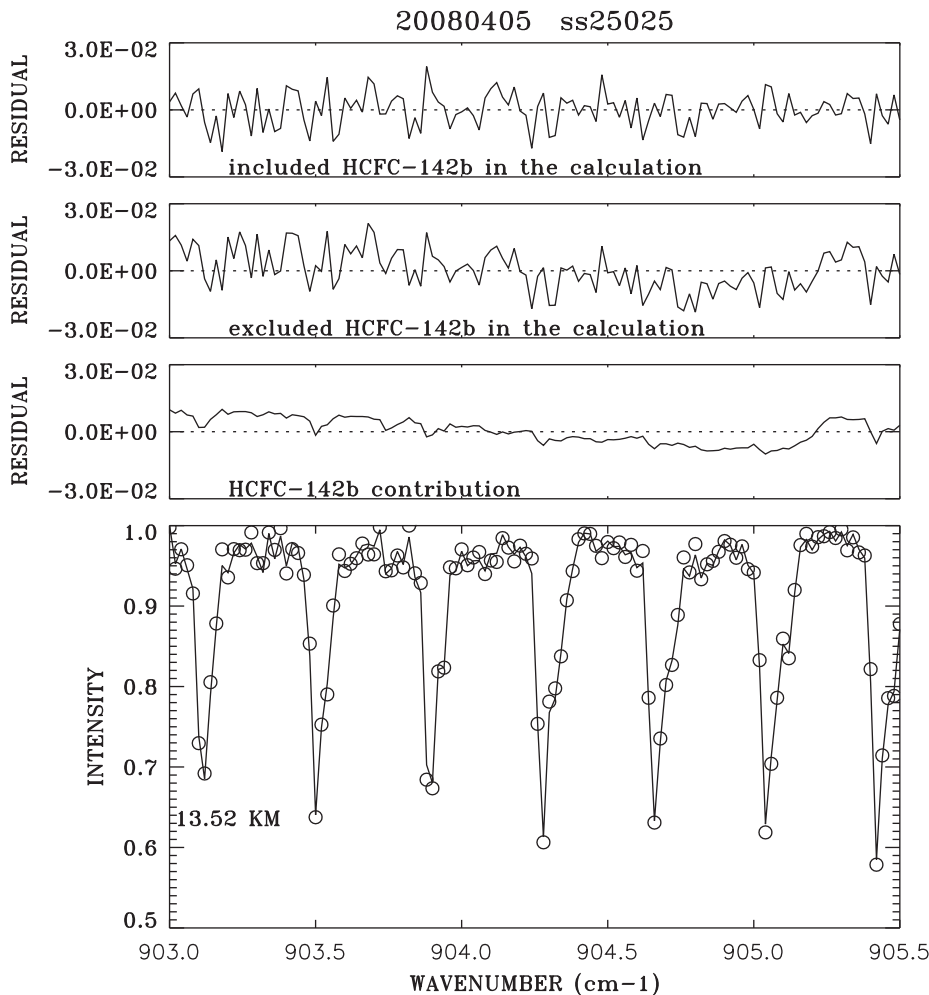


**Fig. 2.** Sample fit to an ACE spectrum (same occultation as displayed in Fig. 1). The top panel shows residuals (measured minus calculated differences) on an expanded vertical scale. In the bottom panel, the solid line shows measured spectra and open circles show calculated intensities. The second residual shows the fit with the VMR of HCFC-142b assumed to zero. The third residual plot is the HCFC-142b contribution calculated as the difference between excluded minus the included HCFC-142b contribution.

time period. Open triangles in the upper panel are the monthly mean mixing ratios (13–16 km) in the northern hemisphere, the vertical lines represent their standard deviations. Solid triangles and vertical lines are used to display the southern hemisphere results. Although the surface time series shows a similar increase rate in both hemispheres, the ACE measurements in both hemispheres are higher than those from the surface stations results by a factor of  $\sim 1.10$  with the southern hemisphere Cape Grim station VMRs lower than those from the northern hemisphere Niwot Ridge station. An interhemispheric difference in monthly mean surface station measurements is consistent with a time series of flask sampling measurements [4,5].

We adopted the empirical expression to determine the time dependence of  $V$  from fits to the ACE and surface station measurement VMR time series,

$$V = a_0 + a_1(t - t_0). \quad (1)$$

In Eq. (1),  $t$  is time and  $t_0$  is the time of the first ACE or surface station measurement. The coefficients  $a_0$  and  $a_1$  and their statistical uncertainties were determined from a least-squares fit to average VMRs from each measurement set. The results of the time series for both are reported in Table 1. We report yearly mean VMRs and the best fit trend derived from the fit to the full time series. Our mean trends of  $4.94 \pm 1.51\% \text{ yr}^{-1}$  for ACE measurements at 25–35°N latitude and  $6.63 \pm 1.23\% \text{ yr}^{-1}$  for 25–35°S latitude are consistent with the increase rate of  $0.6 \text{ pptv yr}^{-1}$  reported by WMO [3]. Surface measurement time series from CMDL and NOAA ESRL stations often show low amplitude seasonal cycles superimposed on the long-term trend [4]. We have not modeled the seasonal variation in fitting the time series, although surface measurements indicate a low amplitude seasonal change is superimposed on the long-term trend.

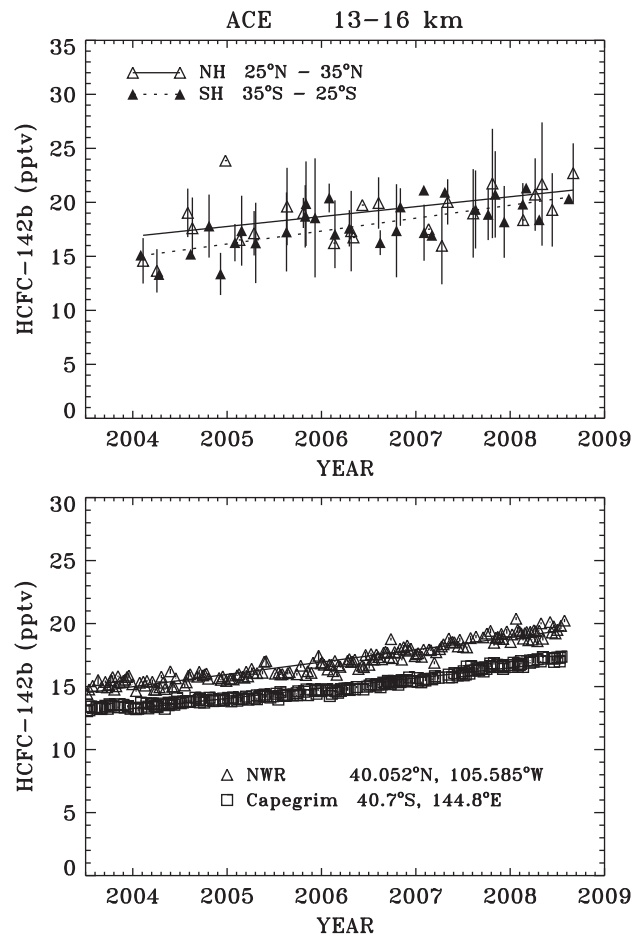


**Fig. 3.** Time series of HCFC-142b ACE and mid-latitude surface stations measurements. Top: 25–35°N latitude ACE monthly average measurements at altitudes of 13–16 km (open triangles) and 25–35°S (black triangles) between February 2004 and August 2008. Vertical lines indicate standard deviations. Lower panel: AGAGE flask sampling measurements from Niwot Ridge and Cape Grim, Tasmania, over a similar time span.

**Table 1**

HCFC-142b VMR (pptv) and trend per year ( $\text{pptv yr}^{-1}$  and  $\% \text{ yr}^{-1}$ ) from best-fits to ACE monthly mean atmospheric spectra at 13–16 km and NOAA ESRL surface station measurements.

Instrument	2004	2005	2006	2007	2008	Trend	Trend
Latitude	(VMR)	(VMR)	(VMR)	(VMR)	(VMR)	( $\text{pptv yr}^{-1}$ )	( $\% \text{ yr}^{-1}$ )
ACE (25–35°N)	$16.909 \pm 3.523$	$18.599 \pm 2.899$	$19.107 \pm 2.754$	$18.587 \pm 3.719$	$21.380 \pm 3.896$	$0.92 \pm 0.28$	$4.94 \pm 1.51$
ACE (25–35°S)	$16.767 \pm 3.069$	$17.953 \pm 3.261$	$17.635 \pm 2.979$	$19.083 \pm 2.80$	$19.765 \pm 1.775$	$1.19 \pm 0.22$	$6.63 \pm 1.23$
Niwot Ridge	$15.459 \pm 0.45$	$16.180 \pm 0.47$	$17.232 \pm 0.60$	$18.415 \pm 0.61$	$19.362 \pm 0.50$	$0.98 \pm 0.02$	$5.73 \pm 0.14$
Cape Grim	$13.697 \pm 0.24$	$14.277 \pm 0.24$	$15.052 \pm 0.35$	$16.140 \pm 0.43$	$17.021 \pm 0.25$	$0.81 \pm 0.01$	$5.46 \pm 0.08$

The VMR for each year is the yearly mean. The ACE time series used 106 occultations to calculate 24 northern hemisphere monthly means, and 123 occultations to compute 30 southern hemisphere monthly means. Trends were derived from a best-fit to the time series with Eq. 1. There were 176 sampling measurements from Niwot Ridge and 222 measurements from Cape Grim. Full time spans used in the fits were February 2004 to August 2008 for ACE in both hemispheres. The time spans of the NOAA ESRL measurements used in the analysis were July 2003–July 2008 for both Niwot Ridge and Cape Grim.

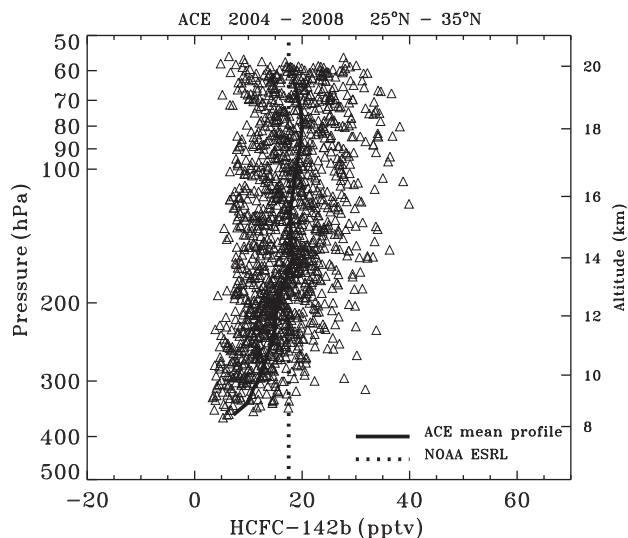
## 5. Error budget

Table 2 provides an evaluation of the random and systematic sources of error in the monthly mean 13–16 km VMR. The spectrum shown in Figs. 1 and 2 was used in the analysis. Random error sources include errors due to noise in the measured spectrum. Random error due to noise in the measured spectrum is estimated to be less than about 1% due to the procedure adopted to eliminate spectra with low signal-to-noise ratios or weak absorption from the database and averaging over monthly time spans. Error in the zenith angle was estimated by increasing the tangent altitudes by 0.2 km at

**Table 2**

Random (R) and systematic (S) sources of error in the monthly mean 13–16 km ACE HCFC-142b retrievals of their estimated relative uncertainties.

Source of error	Type	Relative error (%)
Finite signal-to-noise	R	< 1
Tangent altitude uncertainty	R	0.2
Temperature uncertainty	S	14
Modeling of instrument line shape function	S	0.4
Modeling of interferences	S	20
Forward model approximations	S	2
Retrieval algorithm	S	3
HCFC-142b spectroscopic parameter uncertainties	S	10



**Fig. 4.** Comparison of ACE HCFC-142b VMRs at 25–35°N latitude for the 8–20 km altitude range (plus symbols) with NOAA ESRL measurements from Niwot Ridge for the same time period. A dark black curve indicates the ACE mean profile obtained after interpolation of the individual measurements to the equal altitude spaced grid. The NOAA ESRL Niwot Ridge VMRs were between 15 and 20 pptv, and a dotted vertical line is used to show an approximate mean VMR for the time span. Approximate pressures are shown on the right vertical axis.

all altitudes. The 13–16 km HCFC-142b VMR decreased by 3.2%. There are several significant sources of systematic error. The systematic error in temperature was estimated by increasing the temperature by 2 K at all altitudes. Average HCFC-142b VMRs at 13–16 km altitude decreased by 14%. Systematic errors arise from errors in the forward model including possible inaccuracies in the ray tracing, errors in modeling the ACE instrument line shape function, and biases due to imperfect fitting of interfering absorptions. Ray-tracing calculations have been extensively studied and updated as part of work for the Network of the Detection of Atmospheric Composition Change (NDAAC) [21] and likely introduce a VMR error of less than 1%. As shown in Fig. 2, biases occur due to errors in the fitting of the weak absorption by HCFC-142b as the contribution to the total absorption by the two main interferences  $\text{CO}_2$  and  $\text{HNO}_3$  is much greater than that of HCFC-142b. Although its absorption is much weaker than those by  $\text{CO}_2$  and  $\text{HNO}_3$ , a comparison of profile of  $\text{CCl}_2\text{F}_2$  retrieved with those from ACE version 2.2 results also shows a bias of several percent in the lower atmosphere. The potential systematic biases are due to the uncertainty in the instrument line shape (ILS) function, errors in the forward and retrieval algorithm. We estimated the error in the ILS by modifying the theoretical unapodized function for ACE (which we assumed and was found to fit the ILS of lines in this region well) with an empirical apodization function that decreased linearly from 1.0 at zero optical path difference to a value of 0.9 at the maximum optical path difference for the example case shown in Figs. 1 and 2. The retrieved HCFC-142b VMR at that altitude changed by 0.45%. Forward model approximations and possible errors in the retrieval algorithm were estimated as 2% and 3%, respectively, for example, from retrievals of profiles from the ATMOS FTS. The largest source of systematic error in the retrievals is believed to be possible errors in the assumed HCFC-142b pseudo-lines. As noted earlier, a maximum error of 4% in absorber was found by refitting the laboratory spectra using the final pseudo-linelist. As shown in Table 3 of [10], integrated absorption cross sections assumed in that study and adopted here agreed within ~5% with previously reported temperature dependent measurements for the 870–1030  $\text{cm}^{-1}$  region [12]. We estimate the total error due to possible errors in the assumed spectroscopic parameters as 10%. The total error (random+systematic) for the monthly mean HCFC-142b VMRs reported in Table 1 is ~20%.

As shown in Figs. 1 and 2, the absorption by HCFC-142b is very weak, but by averaging the measurements it is possible to examine the vertical profile. Fig. 4 depicts the results of ACE-retrieved HCFC-142b profiles during 2004–2008 from

latitudes 25–35°N. The plus symbols show each retrieved profile interpolated to a grid with equal altitude intervals. The thick curve represents the mean profile (8–20 km). As can be seen from this profile, the HCFC-142b VMR is approximately constant over the full altitude range. Corresponding approximate pressures are shown on the right vertical axis. Niwot Ridge surface VMRs were between 15 and 20 pptv during this time span, and a dotted vertical line is used to show an approximate surface VMR of 17.5 pptv over this time period. The ACE average vertical profile shows scatter, but is consistent with a nearly constant VMR from 8 to 20 km, above which there is minimal sensitivity. The average tropopause height during the measurement time span was 14.4 km with tropopause heights from NCEP (US National Center of Environmental Protection) measurements varying from 9.91 and 17.85 km. As there is a time lag for transport of surface air to the lower stratosphere of about 4 yr [22], a vertical decrease above the tropopause is expected due to the transport time, but the scatter in the results and the need to average over 4 yr of measurements masks the expected gradient, and we are unaware of any profile predictions available for comparison with our observations. As HCFC-142b is increasing rapidly in the stratosphere, it may not have reached equilibrium [6] and we are unaware of any model predictions of its vertical distribution.

## 6. Summary and conclusions

The first space-based measurements of the trend of the hydrochlorofluorocarbon HCFC-142b ( $\text{CH}_3\text{CClF}_2$ ), a temporary replacement for fully fluorinated chlorofluorocarbons (CFCs) are reported. The trend measurements have been derived from atmospheric solar occultation remote sensing measurements recorded by the Atmospheric Chemistry Experiment (ACE) Fourier transform spectrometer [8]. Monthly average VMRs at 13–16 km altitude were retrieved from ACE atmospheric spectra recorded between February 2004 and August 2008 at latitudes of 25–35°N and 25–35°S. The measured VMRs have been compared with surface sampling measurements obtained over approximately the same time span covering similar latitude bands. The ACE measurements in both hemispheres show similar increase rates, but the scatter in the trend is significantly larger than the surface station measurements and the ACE-measured rate of increase is faster than reported at the surface sites in both hemispheres. Our monthly mean HCFC-142b VMRs are estimated to have an uncertainty of 20%. A mean northern hemisphere profile for the time span shows a near constant VMR at 8–20 km altitude range, consistent on average for the same time span with *in situ* results. The nearly constant vertical VMR profile is consistent with predictions of a long lifetime in the lower atmosphere [3–7]. Although the ACE HCFC-142b retrievals have limited sensitivity because of the weakness of the absorption in the ACE spectra, our results show the potential for remote sensing of atmospheric HCFC-142b, the need for further monitoring of its trend, and the importance of additional investigations of its spectroscopic parameters. Evidence for weak absorption by HCFC-142b has been found in recent ground-based solar spectra recorded from the Jungfraujoch NDACC station (46.5°N latitude, 8.0°E longitude, 3.58 km altitude) [23].

## Acknowledgments

Analysis of the ACE spectra at the NASA Langley Research Center was supported by funding from NASA. The ACE mission is supported primarily by the Canadian Space Agency. Funding for ACE work at York is provided by the UK National Environment Research Council (NERC). E. Mahieu was primarily supported by the Belgian Federal Science Policy Office (AGACC and SECPEA projects), Brussels. We thank S. Montzka of the NOAA ESRL/GMD group (formerly CMDL) for making available a preliminary version of Niwot Ridge HCFC142b time series. We also thank G. Toon of the Jet Propulsion laboratory for access to the “pseudo-line” parameters adopted for analysis of HCFC-142b and  $\text{CCl}_2\text{F}_2$ .

## References

- [1] Montreal Protocol. 1991 Assessment. Report of the technology and economic assessment panel, United Nations Environment Panel, Nairobi, Kenya; December 1991.
- [2] Montreal protocol on substances that deplete the ozone layer, as adjusted and amended by the second meeting of the parties. United Nations Environment Programme, London; 27–29 June 1990.
- [3] Scientific assessment of ozone depletion 2007: World Meteorological Organization global research and monitoring project report no. 50. World Meteorological Organization, Geneva, Switzerland. 572p.
- [4] O'Doherty SO, Cunnold DM, Manning A, Miller BR, Wang RHJ, Krummel PB, et al. Rapid growth of hydrofluorocarbon 134a and hydrochlorofluorocarbons 141b, 142b, and 22 from advanced global atmospheric gases experiment (AGAGE) measurements. *J Geophys Res* 2004;109:D06310.
- [5] Montzka SA, Hall BD, Elkins JW. Accelerated increases observed for hydrochlorofluorocarbons since 2004. *Geophys Res Lett* 2009;36:L03804.
- [6] Lee JM, Sturges WT, Penkett SA, Oram DE, Schmidt U, et al. Observed stratospheric profiles and stratospheric lifetimes of HCFC-142b and HCFC-142b. *Geophys Res Lett* 1995;22:1369–72.
- [7] Dufour G, Boone CD, Bernath PF. First measurements of CFC-113 and HCFC-142b from space using ACE-FTS infrared spectra. *Geophys Res Lett* 2005;32:L15S09.
- [8] Bernath PF, McElroy CT, Abrams MC, Boone CD, Butler M, Camy-Peyret C, et al. Atmospheric chemistry experiment (ACE): mission overview. *Geophys Res Lett* 2005;32:L15S01.
- [9] Coheur PF, Clerbaux C, Colin R. Spectroscopic measurements of halocarbons and hydrohalocarbons by satellite-borne remote sensors. *J Geophys Res* 2003;108(D4):4130. ACH1–14, doi:10.1029/2002JD002649.
- [10] Newnham D, Ballard J. Fourier transform infrared spectroscopy of HCFC-142b. *JQSRT* 1995;53:471–9.

- [11] Paddison SJ, Chen Y, Tschukow-Youx E. An ab initio study of the structures, barriers for internal rotation, vibrational frequencies, and thermodynamic functions of the hydrochlorofluorocarbon  $\text{CH}_3\text{CF}_2\text{Cl}$ . *Can J Chem* 1994;72:561–7.
- [12] Clerbaux C, Colin R, Simon PC, Granier C. Infrared cross sections and global warming potential for 10 alternative hydrocarbons. *J Geophys Res* 1993;98:10491–7.
- [13] Cappelini F, Restelli G. Infrared band strengths and their temperature dependence of the hydrohalocarbons HFC-134a, HFC-152a, HCFC-22, HCFC-123 and HCFC-142b. *Spectrochim Acta* 2002;48a:1127–31.
- [14] Brown AC, Canosa-Mas CE, Parr A, Wayne RP. Laboratory studies of some halogenated ethanes and ethers: measurements of ratios of reactions with OH and of infrared absorption cross-sections. *Atmos Environ* 2000;24A:2499–511.
- [15] Gunson MR, Abbas MM, Abrams MC, Allen M, et al. The atmospheric trace molecule spectroscopy (ATMOS) experiment: deployment on the ATLAS space shuttle missions. *Geophys Res Lett* 1996;23:2332–6.
- [16] Norton RH, Rinsland CP. ATMOS data processing and science analysis methods. *Appl Opt* 1991;30:389–400.
- [17] Carlotti M. Global-fit approach to the analysis of limb-scanning atmospheric measurements. *Appl Opt* 1988;27:2350–4.
- [18] Rothman LS, Jacquemart D, Barbe A, Benner DC, Brown LR, et al. The HITRAN 2004 molecular spectroscopic database 2005. *JQSRT* 2005;96:139–204.
- [19] Rothman LS, Gordon IE, Barbe A, Benner DC, Bernath PF, Birk M, et al. The HITRAN 2008 molecular spectroscopic database. *JQSRT* 2009;110:533–72.
- [20] Boone CD, Nassar R, Walker KA, Rochon Y, McLeod SD, Rinsland CP, et al. Retrievals for the atmospheric chemistry experiment Fourier-transform spectrometer. *Appl Opt* 2005;44:7218–31.
- [21] Meier A, Goldman A, Manning PS, Stephen TM, Rinsland CP, Jones NB, et al. Improvements to air mass calculations from ground-based infrared measurements. *JQSRT* 2004;83:109–13.
- [22] Schoeberl MR, Douglass AR, Boelanski B, Boone C, Walker KA, Bernath P. Estimation of the stratospheric age spectrum from chemical tracers. *J. Geophys Res* 2005;110:D21305 doi:10.1029/2005JD006125.
- [23] HFSJG International Foundation Activity Report, University of Liège; 2008.